SCIENCE CHINA
Chemistry

•ARTICLES•

https://doi.org/10.1007/s11426-019-9705-4

Tweaking the acid-sensitivity of transiently thermoresponsive polyacrylamides with cyclic acetal repeating units

Simon Van Herck & Bruno G. De Geest*

Department of Pharmaceutics, Ghent University, Ghent, Belgium

Received December 10, 2019; accepted February 18, 2020; published online March 13, 2020

Merging the characteristics of thermoresponsive and stimuli-degradable polymers yields so-called transiently thermoresponsive polymers, which can find application for the design of injectable gels, nanoparticles, etc. within a biomedical context. Among these polymers, only a limited number is reported which shows selective degradation under mild acidic conditions. However, extension of the library of transiently thermoresponsive polymers is desired to broadening the biomaterials toolbox to suit specific needs. Three monomers were developed by modification of 2-hydroxyethylacrylamide (HEAm) via tetrahydropyranylation or -furanylation with 3,4-dihydro-2*H*-pyran (DHP), 2,3-dihydrofuran (DHF) or 2,3-dihydro-5-methylfuran (MeDHF). The presence of an acetal or ketal bond provided the monomers a pH-dependent hydrolysis behavior ranging from minutes to days. RAFT polymerisation allowed for the construction of homopolymers with temperature responsive behavior and pH-dependent hydrolysis which was strongly influenced by nature of the monomeric repeating units.

acetals, polyacrylamides, stimuli-responsive

Citation: Van Herck S, De Geest BG. Tweaking the acid-sensitivity of transiently thermoresponsive polyacrylamides with cyclic acetal repeating units. *Sci China Chem*, 2020, 63, https://doi.org/10.1007/s11426-019-9705-4

1 Introduction

The evolution in materials chemistry has led to broad range of materials that hold promise for applications in a drug delivery [1]. Many examples exist of protein therapeutics which are PEGylated to reduce opsonisation and increase circulation time [2,3]. Moreover, polymers can be utilized to encapsulate drugs into nanocarriers [4,5]. Encapsulation of highly potent compounds circumvents the poor aqueous solubility often seen with these compounds and leads to a more advantageous safety profile due to improved pharmacokinetics and pharmacodynamics [6–9]. Despite the vast amount of research in this field, successful clinical translation is rather limited [6].

For drug delivery applications, two classes of polymers have received a formidable amount of attention, being thermoresponsive polymers [10] and stimuli-degradable polymers [11]. Among the temperature-responsive polymers, polymers that exhibit a coil-to-globule transition upon change in temperature, those with a lower critical solution temperature (LCST) have received most attention [10,12–14]. By far the best known examples are poly(*N*-isopropyl acrylamide) (pNIPAm) [15–17] and oligo(ethylene glycol) (meth)acrylate) [18] polymers. Block copolymer systems based on these polymers have the ability to self-assemble into nanostructures upon heating in aqueous environment, thus avoiding the use of organic solvents to form drug delivery vehicles. The main limitation of the above-mentioned polymers is that they lack the property to disassemble, hindering both the release of active compound and the clearance from the body. The hindrance in drug release has given rise to the second type, the stimuli-degradable polymers. Incorporation of functional groups that are sensitive to localized conditions like pH, oxidation/re-

*Corresponding author (email: br.degeest@ugent.be)

duction or specific enzymes can provide on-demand drug delivery [19–22].

A combination of the two responsive properties is provided by so-called transiently thermoresponsive polymers—i.e., polymers that change their conformation in response to temperature, but loose this property as consequence to an alteration in the polymer side chain or backbone induced by a physiologically relevant stimulus rendering them fully hydrophilic [10,23]. This concept allows to start with a soluble polymer that upon temperature increase will self-assemble into a micellar structure able to incorporate a hydrophobic compound and that after endocytosis will become fully soluble irrespective of temperature due to hydrolysis of in the side chains induced by the acidic pH in the endo/lysosomal vesicles.

To allow for endo/lysosomal acidic-pH induced hydrolysis, acetal chemistry has been explored [24]. A large body of research has been devoted to polyacetal/ketal synthesis by step-growth polymerization [25–31], whereas only a limited number of transiently thermoresponsive polymers systems with an acid-dependent degradation have been reported [10,32]. These either consist of a degradable monomer copolymerised with a non-degradable thermoresponsive monomer or do not possess the desirable properties in a biologically relevant window [32,33].

Hence, extending the limited library of currently existing transiently thermoresponsive polymers is needed to obtain polymers with more optimal properties as well as broadening the biomaterials toolbox to suit specific needs. Here we present a new set of transiently thermoresponsive polymers that exhibit LCST behavior and degrade into fully water soluble polymers in response to an acidic stimulus. We build on previous work published by our group on a 3,4-dihydro-2*H*-pyran (DHP) modified acrylamide by extending the modifications with furan acetal and ketal derivatives [34]. A comparative study is performed to investigate the influence of hydrophobic modification on the relevant properties like the phase-transition temperature (for the sake of simplicity denoted as cloud-point temperature, T_{cp}), hydrolysis rate and self-assembly behavior of polymers made thereof.

2 Experimental

2.1 Materials

All chemicals and solvents were obtained from commercial sources and used as perceived unless otherwise noted. 2.2′-azobis(2-methylpropionitrile) (AIBN) as initiator was provided by WAKO Chemicals and purified by recrystallization from diethyl ether prior to use. The RAFT CTA 2-(butylthiocarbonothioylthio)propanoic acid (PABTC) was synthesized according to literature [35,36].

2.2 Instrumentation

All ^{1}H- and ^{13}C-NMR spectra were recorded on a Bruker 300 MHz or 400 MHz FT NMR spectrometer (Germany). Chemical shifts (δ) are provided in ppm relative to TMS. Samples were prepared in given deuterated solvents and their signals referenced to residual non-deuterated signals of the solvent.

ESI-MS was performed on a Waters LCT Premier XETM time of flight (TOF) mass spectrometer (USA) equipped with a standard electrospray ionization and modular LockSpray TM interface. The purity of the products was assessed by high-performance liquid chromatography (HPLC) and photodiode array (PDA) detection (190–400 nm) using a reverse phase column (Phenomenex Luna 3 µm C18 (2), 100 Å, 200 mm) with a linear gradient of 10%–100% B over 9 min, where A is 0.1% formic acid in H_2O and B is 0.1% formic acid in CH_3CN at a flow rate of 0.4 mL/min.

HPLC measurement was performed using a system with an isocratic solvent pump (L-7100, Merck, Hitachi LaChrom, Japan), an autosampler (L-7200, Merck, Hitachi LaChrom) with a loop of 100 µL, a guard column (RP 18e) followed by a reversed phase C18 column (LiChroCart® 125-4, LiChrospher® 100 RP (5 µm)) and a UV-detector (L-7400, Merck, Hitachi LaChrom).

Molecular weight distribution analysis was performed by size exclusion chromatography (SEC) measurements on a Shimadzu 20A system in dimethylacetaminde (DMAc) as solvent containing 50 mM LiBr. The system was equipped with a 20A ISO-pump and a 20A refractive index detector (RID). Measurements were recorded at 50 °C with a flow rate of 0.700 mL/min. Calibration of the 2 PL 5 µm Mixed-D columns was done with poly(methyl methacrylate) (PMMA) standards obtained from PSS Polymer Standards Service GmbH (Mainz, Germany). Samples were run with toluene as an internal standard.

Dynamic light scattering (DLS) was performed on a Zetasizer Nano S (Malvern Instruments Ltd., Malvern, UK) equipped with a HeNe laser (λ=633 nm) and detection at scattering angle of 173°. Cumulants analysis of the data gave the z-average and polydispersity index and data fitting by CONTIN the particle size distribution.

2.3 Methods

Synthesis of N-(2-((tetrahydro-2H-pyran-2-yl)oxy])ethyl)-acrylamide (THPEAm). Camphorsulfonic acid (1.630 g, 7.02 mmol) and *N*-(2-hydroxyethyl)acrylamide (7.5 mL, 70.2 mmol) were dissolved in 100 mL dry dichloromethane (DCM). To this mixture 3,4-dihydro-2*H*-pyran (7.68 mL, 70.2 mmol) was added dropwise at 0 °C. The reaction mixture was stirred at RT under N_2. After 3 h the reaction is quenched by addition of trieyhylamine (TEA). The mixture

was concentrated *in vacuo*, dissolved in ethyl acetate and filtered. The filtrate was concentrated and purified by column chromatography (DCM/EtOAc–80:20+1% TEA) to give 11.9 g (85% yield) of a clear viscous oil. ^{1}H NMR (300 MHz, DMSO-d_6) δ ppm: 8.16 (br.s, 1H), 6.25 (dd, J=17.1, 10.0 Hz, 1H), 6.07 (dd, J=17.1, 2.4 Hz, 1H), 5.57 (dd, J=10.0, 2.4 Hz, 1H), 4.56 (t, J=3.7 Hz, 1H), 3.74 (tt, J=8.0, 3.2 Hz, 1H), 3.64 (dt, J=9.7, 6.0 Hz, 1H), 3.45–3.37 (m, 2H), 3.33–3.21 (m, 2H), 1.82–1.67 (m, 1H), 1.67–1.57 (m, 1H), 1.55–1.35 (m, 4H). ^{13}C NMR (75 MHz, DMSO-d_6) δ ppm: 164.67, 131.73, 125.03, 98.06, 65.41, 61.40, 38.72, 30.20, 25.00, 19.15. ESI-MS calcd for $C_{10}H_{17}NO_3$, m/z =222.1101, found 222.1111 $[M+Na]^+$.

Synthesis of N-(2-((tetrahydro-2H-furan-2-yl)oxy)ethyl) -acrylamide (THFEAm). Camphorsulfonic acid (921.8 mg, 3.968 mmol) and *N*-(2-hydroxyethyl)acrylamide (4.568 g, 39.68 mmol) were dissolved in 80 mL dry DCM. To this mixture 2,3-dihydrofuran (3.0 mL, 39.68 mmol) was added dropwise at 0 °C. The reaction mixture was stirred at RT under N_2. After 3 h the reaction is quenched by addition of TEA. The mixture was concentrated *in vacuo* and purified by column chromatography (Hex/EtOAc–50:50+1% TEA) to give 5.029 g (68% yield) of a clear oil. ^{1}H NMR (400 MHz, DMSO-d_6) δ ppm: 8.11 (s, 1H), 6.24 (dd, J=17.1, 10.1 Hz, 1H), 6.07 (dd, J=17.1, 2.3 Hz, 1H), 5.57 (dd, J=10.1, 2.3 Hz, 1H), 5.11–5.05 (m, 1H), 3.80–3.70 (m, 2H), 3.56 (dt, J=9.9, 5.9 Hz, 1H), 3.41–3.35 (m, 1H), 3.32–3.18 (m, 2H), 1.91–1.81 (m, 2H), 1.80–1.68 (m, 2H). ^{13}C NMR (101 MHz, DMSO) δ ppm: 164.64, 131.73, 125.02, 103.22, 66.17, 65.11, 38.75, 31.81, 23.03. ESI-MS calcd for $C_9H_{15}NO_3$, m/z=208.0944, found 208.0943 $[M+Na]^+$.

Synthesis of N-(2-((2-methyltetrahydrofuran-2-yl)oxy) ethyl)acrylamide (MeTHFEAm). To *N*-(2-hydroxyethyl)acrylamide (8.55 g, 71.3 mmol) dissolved in 300 mL anhydrous DCM were consecutively added molecular sieves followed by 2,3-dihydro-5-methylfuran (5.0 g, 59.4 mmol) and the mixture was cooled on ice. Camphorsulfonic acid (138 mg, 0.59 mmol) was added and the reaction mixture was stirred 30 min on ice followed by 3 h at room temperature. Next, the reaction was quenched with TEA (8.3 mL, 59.4 mmol), filtered, concentrated under reduced pressure and purified by column chromatography (hexane/EtOAc–20:80+1% TEA) to give 6.97 g (58%) of an yellowish oil. ^{1}H NMR (400 MHz, DMSO-d_6) δ ppm: 8.09 (br. s, 1H), 6.23 (dd, J=17.1, 10.1 Hz, 1H), 6.07 (dd, J=17.1, 2.3 Hz, 1H), 5.56 (dd, J=10.1, 2.3 Hz, 1H), 3.82–3.66 (m, 2H), 3.47–3.33 (m, 2H), 3.26–3.18 (m, 2H), 2.01–1.87 (m, 2H), 1.86–1.74 (m, 1H), 1.72–1.61 (m, 1H), 1.33 (s, 3H). ^{13}C NMR (101 MHz, DMSO-d_6) δ ppm: 164.61, 131.78, 124.93, 106.99, 59.25, 39.19, 37.38, 24.02, 21.95. ESI-MS calcd for $C_{10}H_{17}NO_3$, m/z=222.1101, found 222.1122 $[M+Na]^+$.

2.4 Determination of hydrolysis rate of acetal bearing monomers (THPEAm and THFEAm)

Monomer solutions were prepared at 0.5 mg/mL in 100 mM acetate buffer pH 5 and 100 mM phosphate buffer pH 7.4 in triplicate. A trace amount of hydroquinone monomethyl ether (200 ppm) was added to avoid polymerisation. The solutions were stirred at 37 °C. At regular time points samples were taken by diluting 20 μL of the hydrolysis solution into 180 μL 100 mM phosphate buffer pH 7.4 and stored at −18 °C. Prior to injection the samples were diluted 5 times with eluent. Analysis was done by HPLC using water/acetonitrile 60:40 as eluent, with the flow rate set at 0.2 mL/min and detection at 207 nm. Assessment of the hydrolysis rate was done taking the ratio of molar concentrations of the compounds calculated from calibration curves for THPEAm and HEAm (Figure S8).

$$\%\text{hydrolysis}=\frac{[\text{HEAm}]}{([\text{HEAm}]+[\text{HEAmTHP}])}\times 100\,\%$$

2.5 Determination of hydrolysis rate of MeTHFEAm

Monomer solution was prepared at 0.5 mg/mL in 20 mM acetate buffer (pH 5), 20 mM phosphate buffer (pH 7.4) and in 20 mM carbonate buffer (pH 9) in triplicate. A trace amount of hydroquinone monomethyl ether (200 ppm) was added to avoid polymerisation. The solutions were stirred at 37 °C. At regular time points, 4 μL sample was collected and diluted to 200 μL with mobile phase. All samples were immediately stored in the freezer before further quantification by HPLC. HPLC analysis was done using carbonate buffer (pH 9)/acetonitrile–70:30 as mobile phase, flow rate at 0.2 mL/min and detection at 207 nm. Assessment of the hydrolysis rate was done taking the ratio of the AUC for hydrolysis product (HEAm) over the total AUC of hydrolysis product+starting product, according to following equation:

$$\%\text{hydrolysis}=\frac{\text{AUC}_{\text{HEAm}}}{(\text{AUC}_{\text{MeTHFEAm}}+\text{AUC}_{\text{HEAm}})}\times 100\,\%$$

RAFT homopolymerisation of THPEAm. pTHPEAm$_{42}$ and pTHPEAm$_{66}$ were synthesised following the same protocol with only altering the amount of PABTC and AIBN. As an example, the protocol for pTHPEAm$_{42}$ is given here. A Schlenk tube was loaded with THPEAm (600 mg, 3 mmol), 2-(butylthiocarbonothioylthio)propanoic acid (PABTC) (14.35 mg, 0.06 mmol) and AIBN (1.97 mg, 0.012 mmol) and dissolved in anhydrous DMF (2 M). The mixture was degassed by five freeze-vacuum-thaw cycles and immersed in a pre-heated oil bath at 80 °C under vigorous stirring. After 1 h the reaction was quenched by cooling and exposure to air. Samples were taken at regular time point and analysed by ^{1}H NMR to determine monomer conversion. The result-

ing polymer was isolated by repeated precipitations in ice-cold diethyl ether with acetone for re-dissolving the polymer. The precipitated polymer was dried under vacuum to give 300 mg yellow powder. Polydispersity of purified polymer was analysed by size exclusion chromatography (SEC). ^{1}H NMR (300 MHz, DMSO-d_6) δ ppm 4.63 (s, 1H), 3.90 (s, 1H), 3.80 (s, 1H), 3.68–3.32 (m, 4H), 1.65 (d, J=54.7 Hz, 9H).

Conditions for pTHPEAm$_{66}$. THPEAm (600 mg, 3 mmol), 2-propanoic acid butyl trithiocarbonate (7.18 mg, 0.03 mmol) and AIBN (0.988 mg, 0.006 mmol).

RAFT homopolymerisation of THFEAm. pTHFEAm$_{47}$ and pTHFEAm$_{91}$ were synthesised following the same protocol with only altering the amount of PABTC and AIBN. As an example, the protocol for pTHFEAm$_{47}$ is given here. A Schlenk tube was loaded with THFEAm (1 g, 5.4 mmol), 2-propanoic acid butyl trithiocarbonate (25.74 mg, 0.108 mmol) and AIBN (3.547 mg, 0.0216 mmol) and dissolved in anhydrous DMF (2 M). The mixture was degassed with five freeze-vacuum-thaw cycles and immersed in a pre-heated oil bath at 80 °C under vigorous stirring. After 1 h, the reaction was quenched by cooling and exposure to air. Samples were taken at regular time point and analysed by ^{1}H NMR to determine monomer conversion. The resulting polymer was isolated by repeated precipitations in ice-cold diethyl ether with acetone for re-dissolving the polymer. The precipitated polymer was dried under vacuum to give 584 mg yellow powder. Polydispersity of purified polymer was analysed by size exclusion chromatography (SEC). ^{1}H NMR (300 MHz, DMSO-d_6) δ ppm 7.37 (s, 1H), 5.09 (d, J= 5.0 Hz, 1H), 3.76 (t, J=6.3 Hz, 2H), 3.51 (s, 2H), 3.18 (s, 2H), 2.20–1.04 (m, 7H).

RAFT homopolymerisation of MeTHFEAm. pMeTHFEAm$_{43}$ and pMeTHFEAm$_{46}$ were synthesised following the same protocol with only altering the amount of PABTC and AIBN. As an example, the protocol for pMeTHFEAm$_{43}$ is given here. A Schlenk tube was loaded with MeTHFEAm (741 mg, 4 mmol), 2-propanoic acid butyl trithiocarbonate (19.1 mg, 0.08 mmol) and AIBN (2.63 mg, 16 μmol) and dissolved in anhydrous DMF (2 M) containing 10 *V*% pyridine. The mixture was degassed with five freeze-vacuum-thaw cycles and immersed in a pre-heated oil bath at 80 °C under vigorous stirring. After 75 min the reaction was quenched by cooling and exposure to air. Samples were taken at regular time point and analysed by ^{1}H NMR to determine monomer conversion. The resulting polymer was isolated by repeated precipitations in a mixture of ice-cold diethyl ether/hexane with acetone for re-dissolving the polymer. The precipitated polymer was dried under vacuum to give a yellow powder. Polydispersity of purified polymer was analysed by size exclusion chromatography (SEC). ^{1}H NMR (400 MHz, DMSO-d_6) δ ppm 7.37 (s, 1H), 3.87–3.65 (m, 2H), 3.41 (s, 2H), 3.14 (s, 2H), 2.11–1.17 (m, 10H).

2.6 Cloud point determination of homopolymers

Polymer dispersions were made at 5 mg/mL in PBS or saline NH_4OH solution (7.5 mM ammonia+150 mM NaCl) and cooled. The cooled solutions were filtered through a 0.450 μm filter before measurement to remove dust. Scattering intensity and size were measured over a temperature trend with interval of 1 °C by DLS. Three repeated measurements were done at each temperature except for pMeTHFEAm polymers due to sensitivity to hydrolysis.

2.7 Determination of hydrolysis rate of THPEAm homopolymers

pTHPEAm hydrolysis mixtures were prepared by dissolving the polymer in cold buffer. The experiment is started by heating to 37 °C while stirring. A 50 mM acetate buffer pH 5 +1 M NaSCN and 50 mM phosphate buffer pH 7.4+1 M NaSCN were used as testing conditions. At regular time points a 4 mL sample was taken and dialysed against 10 mM NH_4OH solution. All samples were dialysed 4 d during which the medium was frequently refreshed, followed by freeze drying. The freeze-dried samples were dissolved in deuterated methanol for ^{1}H NMR analysis, afterwards methanol was evaporated, and 5 mg/mL sample solutions were made in 50 mM phosphate buffer pH 7.4 for turbidimetry measurement. Measurements were done by 3 repeated heating-cooling cycles and the average was used to plot the graphs.

2.8 Determination of hydrolysis rate of pTHFEAm and pMeTHFEAm

Hydrolysis of pTHFEAm and pMeTHFEAm polymers was monitored by ^{1}H NMR. Polymers were dispersed at 10 mg/mL in deuterated phosphate buffers with pH 5, 7 or 9 and incubated at room temperature. At regular time points measurements were collected.

3 Results and discussion

3.1 Monomer synthesis

Previously, we reported on engineering the water-soluble acrylamide *N*-(2-hydroxyethyl)acrylamide (HEAm), a commercially available hydrophilic monomer, with an acid-sensitive hydrophobic moiety through an acetal using DHP, yielding THPEAm. In our endeavours to design transiently thermoresponsive polymers, the use of acrylamides instead of (meth)acrylates, takes advantage of the presence of the amide moiety which provides the repeating units with a more hydrophilic character through hydrogen bonding with water molecules below the phase transition temperature of the re-

sulting polymers. However, dehydration of the acrylamide side chains on its turn should provide a driving force for coil-to-globule transition above a critical Tcp [14,37]. Here we extended the monomer toolbox by reacting HEAm with respectively 2,3-dihydrofuran (DHF) and 2,3-dihydro-5-methylfuran (MeDHF), yielding *N*-(2-((tetrahydro-2*H*-furan-2-yl)oxy)ethyl)-acrylamide (THFEAm) and *N*-(2-((2-methyltetrahydrofuran-2-yl)oxy)ethyl)acrylamide (MeTHFEAm), respectively (Scheme 1). DHP is a well-known compound from protection group chemistry [38]. It is used as a base-stable protective moiety for hydroxyl groups obtained through tetrahydropyranylation and can be cleaved under acidic conditions due to hydrolysis of the acetal bond. In this context we expanded this approach with two lesser known furan based compounds, which allowed us to investigate the influence of a 5 or 6 member ring (THP vs. THF) and an acetal or ketal bond (THP/THF vs. MeTHF).

All monomers could be obtained through an acid-catalysed acetalization reaction between the hydroxyl group of HEAm and the enol ether in the pyran or furan ring. Reactions were conducted at low temperature using equimolar amounts of both reagents and a catalytic amount of camphorsulfonic acid (CSA). The reaction yields strongly differed based on the nature of the chemical bond, with the lowest yield obtained for the more acid-sensitive ketal linkage (MeTHFEAm, 58%). NMR spectra of the purified monomers are provided in Figures S1–S6 (Supporting Information online). In an attempt to further optimise monomer synthesis an alternative reaction was tested using an organocatalyzed acetalization described by Kotke *et al.* [39,40]. Their "Schreiner's Catalyst" is an electron-deficient thiourea able to catalyse the acetal formation under non-acidic conditions, thereby avoiding the equilibrium status of the acetalization which lowers product yield. However, no advantage was observed compared to the acid-catalysed reaction, at least not in our hands. Reactions done in dilution media showed extremely low kinetics and the use of a large excess of vinyl ether yielded side reactions. This route was therefore not investigated further.

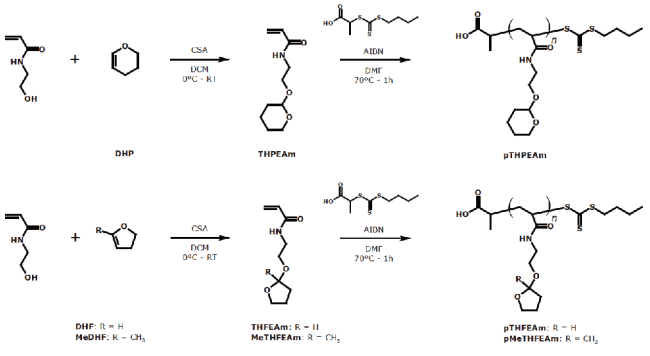

Scheme 1 Monomer synthesis and RAFT polymerization of THPEAm, THFEAm and MeTHFEAm.

3.2 Acid catalysed monomer degradation

Acid catalysed hydrolysis of all three monomers was confirmed by ^{1}H NMR analysis (Figure 1), showing a shift of the acetal proton (b) to a lactol proton (c) for THPEAm and THFEAm and the disappearance of the furan ring (f) for MeTHFEAm. The pH-dependent hydrolysis rate of the different functionalities was evaluated by HPLC analysis in response to aqueous buffers at pH 5, 7.4 and 9 representing lysosomal, physiological and basic pH conditions, respec-

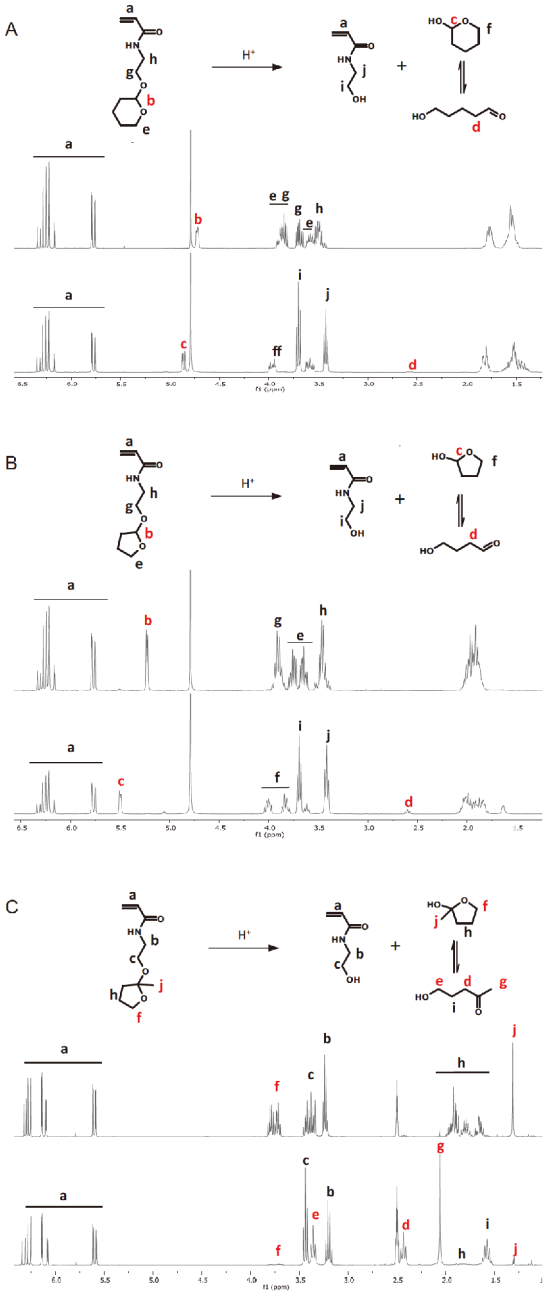

Figure 1 ^{1}H NMR (D_2O or DMSO-d_6) of modified acrylamide monomers: THPEAm (A), THFEAm (B) and MeTHFEAm (C) before and after hydrolysis in acidic conditions. Most relevant proton peaks for identification of the hydrolysis products are marked in red (color online).

tively (Figure 2). Although THPEAm and THFEAm bear great similarity in structure, a clear difference was observed in degradation rate under acidic conditions (i.e., pH 5 buffer). THFEAm has a half-life of approximately 5 h, while this was 19 h for THPEAm. Both the difference in hydrophobicity and/or ring strain could explain this behavior. Figure 1(b) shows that the higher ring strain of the 5-membered lactol ring formed during hydrolysis of THFEAm causes an increased amount of ring opening and formation of the corresponding aldehyde, 4-hydroxybutanal (shift d). This on its turn could shift the equilibrium towards hydrolysis as there is a decreased amount of direct hydrolysis product, i.e., the lactol. Hydrolysis of THPEAm (Figure 1(a)) only yields up to 2.5% of the 5-hydroxypental, while up to 15% of 4-hydroxybutanal is formed upon THFEAm (Figure 1(b)) hydrolysis. The switch from an acetal to a ketal bond for MeTHFEAm results in a dramatic increase in hydrolysis rate. Full hydrolysis of MeTHFEAm was immediate in pH 5 buffer and occurred within the hour at pH 7. Even at pH 9 hydrolysis was rather fast with a half-life around 9 h, providing proof for the instability of the ketal group of MeTHFEAm in aqueous environment. This is in sharp contrast with the acetal containing monomers, THPEAm and THFEAm, that show only limited hydrolysis at pH 7 after several days. The much faster hydrolysis rate is known for ketal bonds and is additionally driven by the equilibrium between cyclic (Figure 1(c) shift f) or linear state (Figure 1(c) shift d/g) of the hydrolysis product, being predominantly the linear 5-hydroxy-2-pentanone [41].

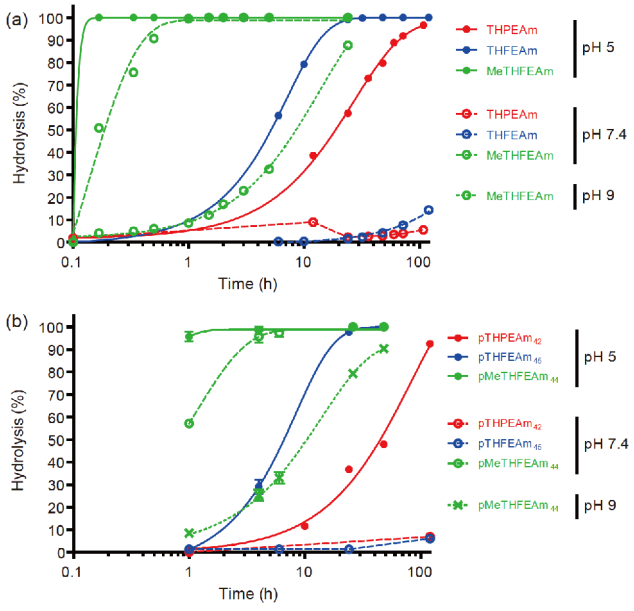

(c)

	$t_{1/2}$		
	pH 5	pH 7	pH 9
THPEAm	19 h	971 h	–
THFEAm	5 h	529 h	–
MeTHFEAm	2 min	10 min	9 h
$pTHPEAm_{42}$	48 h	–	–
$pTHFEAm_{50}$	7 h	–	–
$pMeTHFEAm_{43}$	12 min	50 min	14 h

Figure 2 pH-Dependent hydrolysis profiles of modified acrylamide monomers analysed by HPLC (a) and homopolymers analysed by ^{1}H NMR (b). (c) Relative hydrolysis rates of monomers and homopolymers given as the half-life as a function of pH (color online).

3.3 Polymerization and characterization

Homopolymers of the three acrylamide monomers were synthesised by reversible addition-fragmentation chain transfer (RAFT) polymerization using PABTC as chain transfer agent (CTA), aiming at a degree of polymerisation (DP) of 50 and 100 (Scheme 1 and Table 1). Due to the extreme sensitivity of MeTHFEAm to degradation of the MeTHF moiety, pyridine was added as a base to protect the monomer against hydrolysis. Pyridine was selected over other organic bases such as TEA or DBU as the latter two either stopped polymerisation at low conversion or inhibited polymerisation all together. As an example, the ^{1}H NMR spectra of the purified polymers are shown in Figures S8–S10. Monomer conversion was monitored over time during polymerisation to analyse the effect of functionalisation on the polymerisation kinetics (Figure 3 and Figures S11–S13). From the kinetics of monomer consumption, it is clear that polymerisation of THFEAm is faster compared to THPEAm and MeTHFEAm. Although initial polymerisation rates for THPEAm and THFEAm are fairly similar, at high conversion, the polymerisation rate of THPEAm is markedly slower. This can possibly be linked to steric effect or to viscosity related effects, with higher viscosity for the bulkier THPEAm. Structural effects are even more pronounced at monomer:CTA ratios of 100:1. With both THPEAm and MeTHFEAm showing a delayed initiation and a much slower polymerisation rate compared to THFEAm.

3.4 Evaluation thermoresponsive properties

The thermoresponsive properties of the homopolymers were measured by DLS at polymer concentrations of 5 mg/mL in phosphate buffered saline (PBS; pH 7.4, 0.15 M NaCl) or in a saline ammonia buffer (0.1% NH_4OH+0.15 M NaCl) (Figure 4, Table 1 and Figure S14). All polymers showed a temperature-induced phase transition below physiological temperature. Above this T_{cp} polymers, formed large insoluble aggregates in aqueous medium due to transition into fully hydrophobic polymer chains. As seen from the T_{cp} values in Table 1 as well as in Figure 4, the modification had a strong effect on the T_{cp}, with values well below room

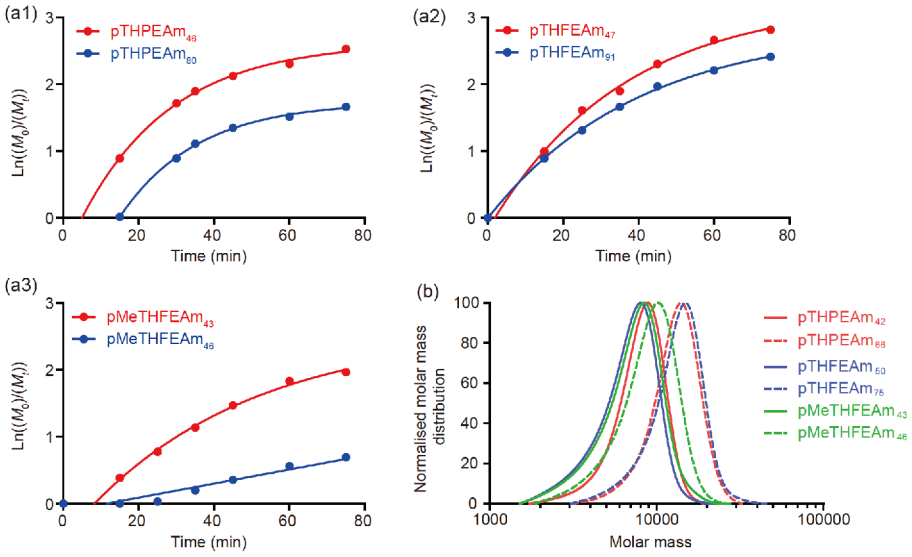

Figure 3 Kinetics plots of polymerisation of THPEAm (a1), THFEAm (a2) and MeTHFEAm (a3) via RAFT polymerisation. (b) Molar mass distribution profiles of purified homopolymers analysed by size exclusion chromatography in DMAc (color online).

Table 1 Summary of polymerization conditions and characterization of synthesized homopolymers

Polymer	CTA	M (eq. to CTA)	Solvent	Temp. (°C)	Time (h)	Conv. (%)[a)]	DP from conv.	M_n^{sec} (kD)[b)]	M_n^{theor} (kD)[a)]	Đ[b)]	T_{cp} (°C)
$pTHPEAm_{42}$	PABTC	50	DMF	80	1 h	84	42	7.4	8.6	1.12	8 [c]
$pTHPEAm_{66}$	PABTC	100	DMF	80	1 h	66	66	12.1	13.4	1.12	6 [c]
$pTHFEAm_{50}$	PABTC	50	DMF	80	75 min	94	47	6.1	8.9	1.17	32 [c]
$pTHFEAm_{75}$	PABTC	100	DMF	80	75 min	91	91	12.2	17.1	1.14	27 [c]
$pMeTHFEAm_{42}$	PABTC	50	DMF+10 V% pyridine	80	75 min	84	42	6.4	8.6	1.19	29 [d)]
$pMeTHFEAm_{46}$	PABTC	100	DMF+10 V% pyridine	80	75 min	46	46	8.0	9.4	1.18	29 [d]

a) Calculated based on ^{1}H NMR spectroscopy data. b) Determined by SEC in DMAc using PMMA for calibration. c) Determined by DLS at 5 mg/mL in PBS. d) Determined by DLS at 5 mg/mL in 10 mM NH_4OH solution+150 mM NaCl.

temperature for pTHPEAm and above room temperature for pTHFEAm and pMeTHFEAm. Although this was never directly investigated, different experimental observations suggest the larger 6-membered pyran ring to be much more hydrophobic, resulting in a lower T_{cp}. Within the same modification, some influence of the chain length on the T_{cp} was observed albeit with a minimal shift. In general, an increase in degree in polymerization resulted in a decrease in T_{cp} due to a more hydrophobic nature of the polymer. This is in line with earlier observations by us on the influence on hydrophobic block length on the T_{cp} for thermoresponsive block copolymers [7,34,42].

The pH-dependent hydrolysis was evaluated for the homopolymers by ^{1}H NMR and revealed a similar trend as observed for the corresponding monomers, showing immediate degradation of the ketal side chain in pMeTHFEAm, both at pH 5 and pH 7 (Figure 1(B)). The degradation half-life for pTHFEAm was in the same range as the THFEAm monomer. This was not the case for pTHPEAm which exhibited a half-life of 48 h, compared to 19 h for the THPEAm monomer (Figure 1(C)). The decrease in hydrolysis rate at pH 5 observed for pTHPEAm can be attributed to the limited aqueous solubility of the polymer with decreased accessibility of water molecules to the collapsed polymer coils above its T_{cp}. The transiently thermoresponsive behavior—i.e., a gradual shift in T_{cp} upon hydrolysis of the pending THP moieties—was investigated by turbidimetry on a colloidal suspension of pTHPEAm at 37 °C (Figure 5 and Figure S15). A clear shift in T_{cp} was found which proves that pTHPEAm loses its hydrophobic properties to become fully soluble, irrespective of temperature. A detailed investigation of the transiently thermoresponsive behavior was not performed for the other polymers due to practical considerations, with pMeTHFEAm hydrolysis to fast and pTHFEAm having a too high T_{cp} at the start. Too high in this context indicates too close to physiological temperature.

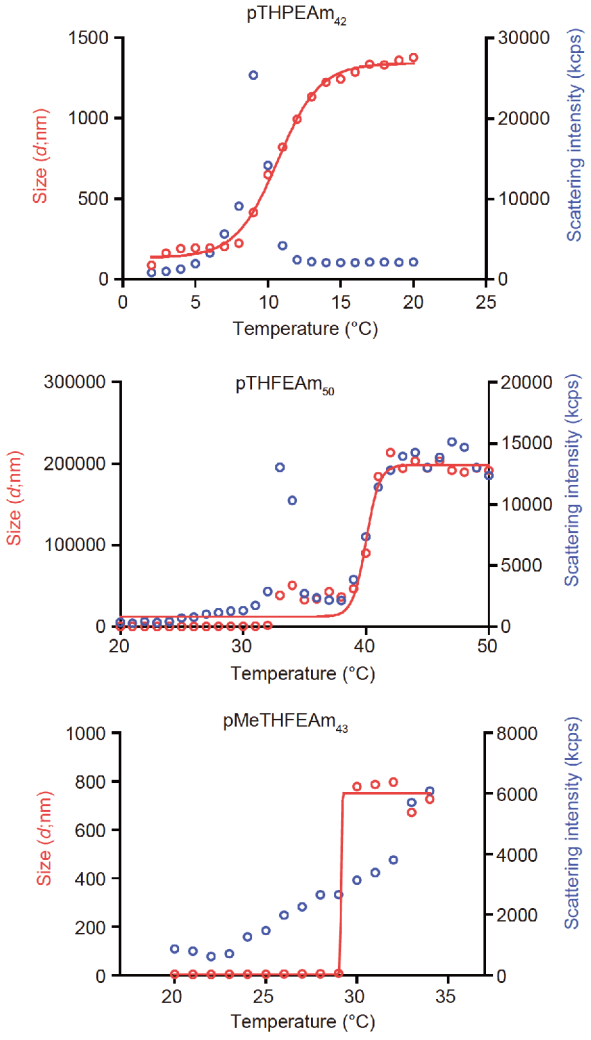

Figure 4 Mean particle diameter (red) and scattering intensity (blue) profiles in function of temperature of homopolymers with targeted DP of 50 analysed by DLS at 5 mg/mL in PBS or saline NH_4OH buffer (color online).

4 Conclusions

Summarizing, cyclic acetal and ketal-functionalized acrylamide monomers were obtained through the modification of the hydrophilic 2-hydroxyethyl acrylamide (HEAm). All monomers could be polymerised by RAFT yielding well defined homopolymers and block copolymers with transient thermoresponsive behavior. Monomers and polymers all showed a pH-dependent hydrolysis due to the presence of the acetal/ketal bond, with accelerated hydrolysis at endosomal pH. Phase transition temperatures strongly varied with modification and chain length of the hydrophobic segment. The more hydrophobic THPEAm polymers resulted in T_{cp} values well below room temperature while these were much higher for THFEAm and MeTHFEAm polymers. We anticipate this work provides a rational base for the design of supramolecular materials containing transiently responsive polymeric building blocks.

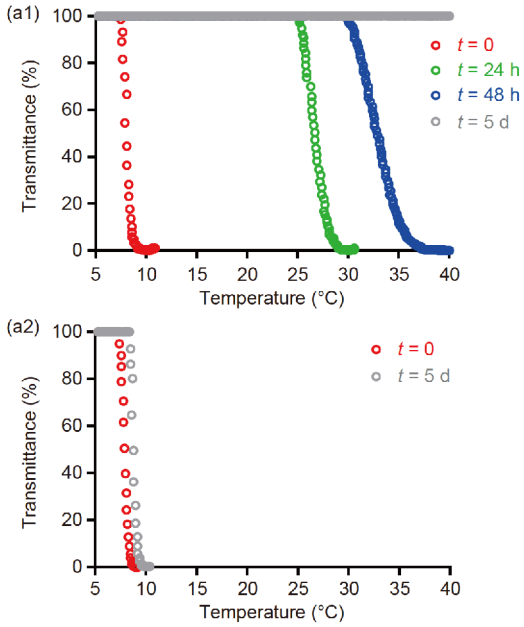

Figure 5 Transmittance profiles of $pTHPEAm_{42}$ dispersions in function of temperature at different time points during hydrolysis at pH 5 (a1) and pH 7.4 (a2) analysed by turbidimetry (color online).

Acknowledgements This work was supported by Ghent University through the BOF-GOA grant scheme.

Conflict of interest The authors declare that they have no conflict of interest.

Supporting information The supporting information is available online at http://chem.scichina.com and http://link.springer.com/journal/11426. The supporting materials are published as submitted, without typesetting or editing. The responsibility for scientific accuracy and content remains entirely with the authors.

1 Ringsdorf H. *J Polym Sci C Polym Symp*, 2007, 51: 135–153
2 Harris JM, Chess RB. *Nat Rev Drug Discov*, 2003, 2: 214–221
3 Owensiii D, Peppas N. *Int J Pharm*, 2006, 307: 93–102
4 Davis ME, Chen ZG, Shin DM. *Nat Rev Drug Discov*, 2008, 7: 771–782
5 Moses MA, Brem H, Langer R. *Cancer Cell*, 2003, 4: 337–341
6 Louage B, De Wever O, Hennink WE, De Geest BG. *J Control Release*, 2017, 253: 137–152
7 Louage B, Zhang Q, Vanparijs N, Voorhaar L, Vande Casteele S, Shi Y, Hennink WE, Van Bocxlaer J, Hoogenboom R, De Geest BG. *Biomacromolecules*, 2015, 16: 336–350
8 Kasmi S, Louage B, Nuhn L, Van Driessche A, Van Deun J, Karalic I, Risseeuw M, Van Calenbergh S, Hoogenboom R, De Rycke R, De Wever O, Hennink WE, De Geest BG. *Biomacromolecules*, 2016, 17: 119–127
9 Shi Y, van der Meel R, Theek B, Oude Blenke E, Pieters EHE, Fens MHAM, Ehling J, Schiffelers RM, Storm G, van Nostrum CF, Lammers T, Hennink WE. *ACS Nano*, 2015, 9: 3740–3752
10 Vanparijs N, Nuhn L, De Geest BG. *Chem Soc Rev*, 2017, 46: 1193–1239
11 Tong R, Tang L, Ma L, Tu C, Baumgartner R, Cheng J. *Chem Soc Rev*, 2014, 43: 6982–7012
12 Roy D, Brooks WLA, Sumerlin BS. *Chem Soc Rev*, 2013, 42: 7214–7243
13 Stuart MAC, Huck WTS, Genzer J, Müller M, Ober C, Stamm M, Sukhorukov GB, Szleifer I, Tsukruk VV, Urban M, Winnik F, Zau-

scher S, Luzinov I, Minko S. *Nat Mater*, 2010, 9: 101–113
14 Gil E, Hudson S. *Prog Polym Sci*, 2004, 29: 1173–1222
15 Zhang Z, Maji S, da Fonseca Antunes AB, De Rycke R, Hoogenboom R, De Geest BG. *Angew Chem Int Ed*, 2016, 55: 7086–7090
16 Schild HG. *Prog Polym Sci*, 1992, 17: 163–249
17 Yin L, He C, Huang C, Zhu W, Wang X, Xu Y, Qian X. *Chem Commun*, 2012, 48: 4486
18 Lutz JF. *J Polym Sci A Polym Chem*, 2008, 46: 3459–3470
19 Mura S, Nicolas J, Couvreur P. *Nat Mater*, 2013, 12: 991–1003
20 Tang L, Zheng Y, Melo MB, Mabardi L, Castaño AP, Xie YQ, Li N, Kudchodkar SB, Wong HC, Jeng EK, Maus MV, Irvine DJ. *Nat Biotechnol*, 2018, 36: 707–716
21 Liu B, Thayumanavan S. *J Am Chem Soc*, 2017, 139: 2306–2317
22 Zheng L, Zhang X, Wang Y, Liu F, Peng J, Zhao X, Yang H, Ma L, Wang B, Chang C, Wei H. *Biomacromolecules*, 2018, 19: 3874–3882
23 Zhang Z, Li H, Kasmi S, Van Herck S, Deswarte K, Lambrecht BN, Hoogenboom R, Nuhn L, De Geest BG. *Angew Chem Int Ed*, 2019, 58: 7866–7872
24 Binauld S, Stenzel MH. *Chem Commun*, 2013, 49: 2082
25 Jain R, Standley SM, Fréchet JMJ. *Macromolecules*, 2007, 40: 452–457
26 Heffernan MJ, Murthy N. *Bioconjugate Chem*, 2005, 16: 1340–1342
27 Murthy N, Xu M, Schuck S, Kunisawa J, Shastri N, Fréchet JMJ. *Proc Natl Acad Sci USA*, 2003, 100: 4995–5000
28 Shenoi RA, Narayanannair JK, Hamilton JL, Lai BFL, Horte S, Kainthan RK, Varghese JP, Rajeev KG, Manoharan M, Kizhakkedathu JN. *J Am Chem Soc*, 2012, 134: 14945–14957
29 Lingier S, Nevejans S, Espeel P, De Wildeman S, Du Prez FE. *Polymer*, 2016, 103: 98–103
30 Delplace V, Nicolas J. *Nat Chem*, 2015, 7: 771–784
31 Wang Y, Huang D, Wang X, Yang F, Shen H, Wu D. *Biomater Sci*, 2019, 7: 3238–3248
32 Vanparijs N, De Coen R, Laplace D, Louage B, Maji S, Lybaert L, Hoogenboom R, De Geest BG. *Chem Commun*, 2015, 51: 13972–13975
33 Zou Y, Brooks DE, Kizhakkedathu JN. *Macromolecules*, 2008, 41: 5393–5405
34 Van Herck S, Van Hoecke L, Louage B, Lybaert L, De Coen R, Kasmi S, Esser-Kahn AP, David SA, Nuhn L, Schepens B, Saelens X, De Geest BG. *Bioconjugate Chem*, 2018, 29: 748–760
35 Ferguson CJ, Hughes RJ, Nguyen D, Pham BTT, Gilbert RG, Serelis AK, Such CH, Hawkett BS. *Macromolecules*, 2005, 38: 2191–2204
36 Van Herck S, Hassannia B, Louage B, Pita Compostizo R, De Coen R, Vanden Berghe W, Vanden Berghe T, De Geest BG. *Eur Polym J*, 2019, 110: 313–318
37 Gibson MI, O'Reilly RK. *Chem Soc Rev*, 2013, 42: 7204–7213
38 Wuts, P. G. M, Greene, T. W. *Greene's Protective Groups in Organic Synthesis*. 4th ed. Hoboken: John Wiley & Sons, Inc., 2006
39 Kotke M, Schreiner PR. *Tetrahedron*, 2006, 62: 434–439
40 Kotke M, Schreiner PR. *ChemInform*, 2007, 38: 779–790
41 Deslongchamps P, Dory YL, Li S. *Tetrahedron*, 2000, 56: 3533–3537
42 Kasmi S, Louage B, Nuhn L, Verstraete G, Van Herck S, van Steenbergen MJ, Vervaet C, Hennink WE, De Geest BG. *Polym Chem*, 2017, 8: 6544–6557